

A Control Topology to Magnify VSC Coupled Weak Grids Performance with Self-Synchronization Capability

Valluri Aravind¹, A. Durga Prasad²P.G. Student, Department of Electrical & Electronics Engineering, Sir C.R.Reddy College of Engg., Eluru, India¹Assistant Professor, Department of Electrical & Electronics Engineering, Sir C.R.Reddy College of Engg., Eluru, India²

ABSTRACT: This paper scrutinize a new course of scenario for a weak grid is to make possible the interfacing of voltage source converters (VSCs) more adequate and to enhance performance of weak grid by damping power and frequency oscillations. To mitigate power and frequency oscillations, a linear controller and non-linear controller is used based on droop characteristics. Here the non-linear controller has cascaded angle, power loops for frequency and angle regulation. The controller provides new control tactic for VSC to damp power and frequency oscillations by accordingly synchronizing the VSC to grid. The linear controller can also be applicable for both islanded and grid connected operation without reconfiguration. The controller endeavours a steady and invariable operation. And also investigation was carried out on system performance at low and high-power references, transition to islanding, self-synchronization. Simulation of the recommended controller was simulated in MATLAB/SIMULINK software. The Secured Simulation results validate that the proposed non-linear controller intensifies the system under unusual disturbances and shows the impressive working of the controller.

KEYWORDS: Distributed generation, linear control, Power damping, Voltage source converter (VSC), Weak grid.

I. INTRODUCTION

Utility restructuring, technology evolution, public environmental policy, and an enlarging electricity market are allowing the impetus for Distributed Generation units [1] to develop into an foremost energy option today. Now-a-days, there is an intensive focus on renewable energy development as a solution to the world's energy needs and to reduce carbon emissions. Many renewable generators are coupled with power electronics, predominantly DC sources such as PV. Integration of DG units to smart grids is a major problem. But VSC's are the better solution for integration of DG units to weak grids. VSC's are the main technology for integrating the renewable and unblemished energy sources to grids [1]-[6]. Vector control [2]-[4] and direct power control [5], [6] are the main controlling topologies for VSC. In order to obtain current and voltage in a synchronously rotating reference frame, a phase locked loop (PLL) is needed. But, during transients PLL affects the system stability. To overcome difficulties associated with vector control of VSCs connected to very weak grids, the concept of power synchronization has been presented in and to provide synchronization [7] with grid in steady-state similar to a synchronous generator (SG). The weak ac grids encounter more problems when connecting DG's. The grid connected VSC supplying a local load is shown in following fig. 1. Here it has two controller's namely linear power-damping/synchronizing controller and supplementary non-linear controller. The linear power-damping and synchronizing controller automatically synchronizes VSC's to weak grids and supplementary non-linear controller will assist the linear controller under non-linear disturbances such as self-synchronization [9], disturbances in grid frequency and angle, high power injection in very weak grids and fault-ride-through conditions.

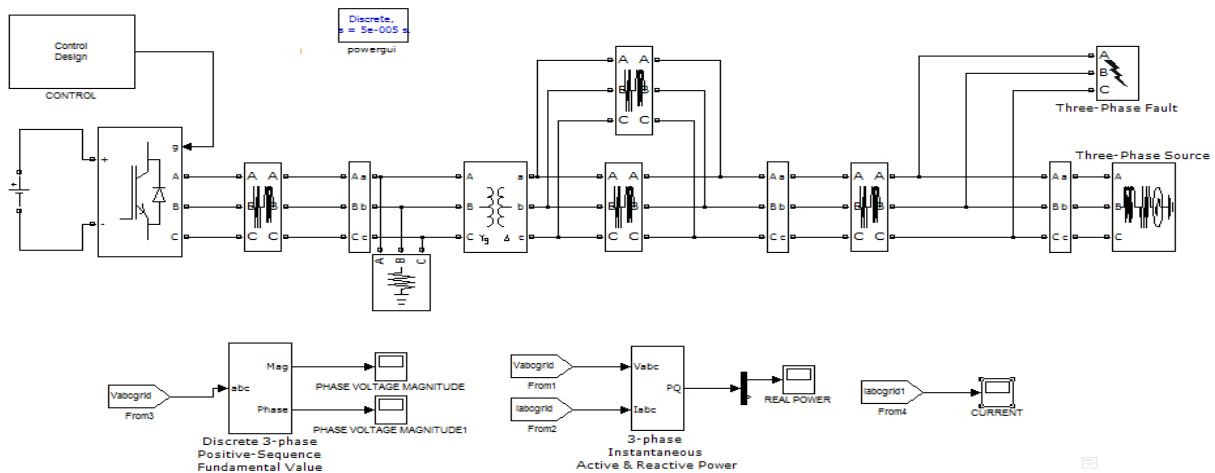


Fig.1. System Model of a grid-connected VSC

The above Fig.1 shows the configuration of the simulated system. The system is composed of a 7.0 MW VSC, filter, local load, transformer and an interface line connecting the VSC to a grid. It is worth to mention that the impedance is the equivalent impedance of the stiff source referred to the distribution level.

II. PROPOSED SCHEME

This paper mainly focuses on improvement of non-linear power damping controller to integrate VSC's to weak grids. It has linear power-damping/ synchronizing controller and non-linear power damping controller. The reference frequency (ω_{set}) in the frequency loop is set equal to the grid frequency and the VSC gives the reference power (P_{set}) in steady state conditions.

The balanced real power is analysed by the following

$$P = \frac{E}{R^2 + X^2} (XV_L \sin \delta + R(E - V_L \cos \delta)) \quad (1)$$

The above equation states that the real power that can be emitted from a VSC is margined. And the SCR capacity can be determined as follows

$$SCR = \frac{\text{short circuit capacity}}{\text{rated capacity}} \quad (2)$$

Where short circuit capacity (S_{sc}) is given by

$$S_{sc} = \frac{E_0^2}{Z} \quad (3)$$

Z is the circuit equivalent Thevenin impedance. This implies that the weaker the grid, the lower the power transfer capacity of the line. In a weak grid with, the theoretical maximum power transfer capacity is 1.0 p.u.

To get rid of the switching effect superimposed on real power, a low-pass filter can be added and purified power is passed to the controller. The power damping control law for a VSC is proposed as follows:

$$\frac{d\Delta\omega}{dt} = -K_p K_f K_d (\omega - \omega_{set}) - K_p K_f \delta - K_p (P - P_{set}) \quad (4)$$

The following two powers weaken load angle and frequency disturbances across an equilibrium point and synchronize the VSC with the grid. Because of the inbuilt frequency and angle loops of the VSCs, the use of the PLL in steady-state

International Journal of Innovative Research in Science, Engineering and Technology

(An ISO 3297: 2007 Certified Organization)

Website: www.ijirset.com

Vol. 6, Issue 1, January 2017

operation and under several transient conditions is eliminated. The damping and the synchronizing power components are expressed as

$$\text{Damping power} = \Delta P_{damp} = -K_f K_P \tag{5}$$

$$\text{Synchronizing power} = \Delta P_{synch} = -K_d \Delta \delta \tag{6}$$

It is important to take into account that the VSC's frequency and angle are internally available; therefore, there is no need for a PLL in steady-state operation and several transient conditions.

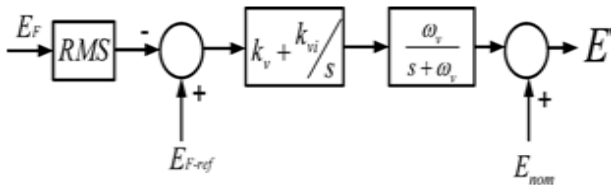


Fig.2. Control Topology for Output Voltage Control P-V Bus.

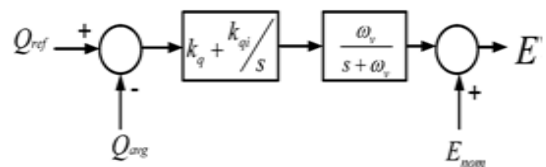


Fig.3. Control Topology for Output Voltage Control P-Q Bus

It provides different control strategy for output voltage to PV and PQ bus. It is shown in Fig.2. Fig.3 also, it has a voltage amplitude controller which provides specific control depending on type of bus.. the angle and frequency loops provide synchronizing and damping power components for the VSC to track frequency and angle deviations of the grid and automatically synchronizes with grid. Depending on the frequency error only the reference of the load angle is found and the real power reference is obtained as the function of load angle error.

III. SYSTEM MODELLING

In this paper, a two-level topology with cooperative nonlinear and linear controllers is developed. The first level is a power synchronizing-damping controller and the second level is a nonlinear controller and the following description analyses the functioning of linear and non-linear power damping controller under disturbance conditions:

➤ Linear controller:

Here the first scenario of action is a linear power-damping and synchronizing controller which automatically synchronizes a VSC to a grid by initiates damping and synchronizing power components, and validates adequate full power injection even under very weak grid conditions. The controller adopts cascaded angle, frequency and power loops for frequency and angle regulation.

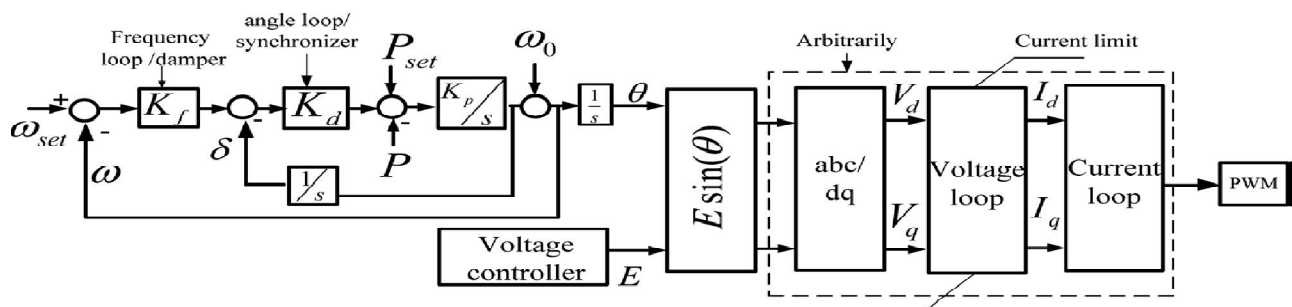


Fig. 4 Proposed linear control scheme

The controller emulates the dynamic performance of synchronous machines, which eases grid integration and provides a virtual inertia control framework for VSCs to damp power and frequency oscillations.

International Journal of Innovative Research in Science, Engineering and Technology

(An ISO 3297: 2007 Certified Organization)

Website: www.ijirset.com

Vol. 6, Issue 1, January 2017

The above fig. 4 shows the linear power damping controller. Although the linear controller offers stable and smooth operation in many cases, it cannot ensure system stability in weak grids, where sudden large disturbances rapidly drift system dynamics to the nonlinear region which is rectified by the following non-linear controller.

➤ Nonlinear Controller:

To overcome the above mentioned difficulty, a supplementary nonlinear controller is developed to assist the linear controller and enhance system performance under large-signal nonlinear disturbances, such as self-synchronization, disturbances in grid frequency and angle, high power injection in very weak grids and fault-ride-through conditions in such situations here come non-linear power damping controller which assists linear controller. The following fig. 5 shows the non-linear power damping controller.

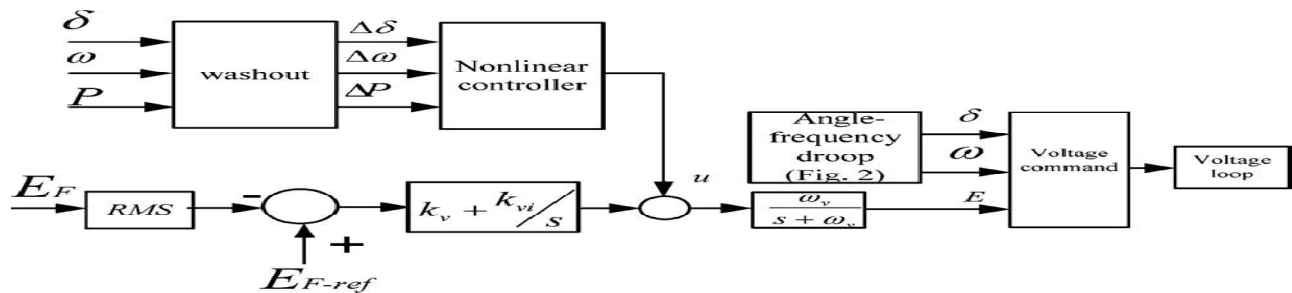


Fig.5. Non-linear power damping controller

Here we will analyze the small-signal stability of a grid-connected VSC is explained. In order to assess the system dynamic behaviour in a powerless grid. The three-phase power system mainly contains a converter and its controller, RL filter, transmission line and infinite grid. Considering VSC as ideal, the controller order is evenly balanced by the VSC local load voltage. Therefore, it is capable of modeling the VSC and PWM block by an average voltage approach. The parameters of the system are presented in Table 1. The obtained model of the VSC and its controller can be obtained as follows.

The load angle dynamic equation is represented as follows and frequency dynamic expression is given by equation (4) and here Δp is given by following expressions

$$\Delta \dot{\delta} = \Delta \omega \tag{7}$$

$$\Delta P = \frac{\partial P}{\partial \delta} \Delta \delta + \frac{\partial P}{\partial E_F} \Delta E_F \tag{8}$$

The voltage loop dynamic expression is given by

$$\Delta \dot{E} = -\omega_v \Delta E + \omega_v \Delta v - w_v k_v \Delta E_F \tag{9}$$

$$\Delta \dot{v} = -K_{vi} \Delta E_F \tag{10}$$

Where v is the output of the integrator, and EF is the filter voltage amplitude expressed by

$$\Delta E_F = \frac{E_F \Delta E_{Fd} + E_{Fq0} \Delta E_{Fq}}{E_{F0}} \tag{11}$$

$$\Delta E_{Fd} = L_c \frac{d\Delta i_d}{dt} + R_c \Delta i_d - \omega_0 L_c \Delta i_q \tag{12}$$

$$\Delta E_{Fq} = L_c \frac{d\Delta i_q}{dt} + R_c \Delta i_q - \omega_0 L_c \Delta i_d \tag{13}$$

The current dynamics in the dq reference-frame are given by

$$\frac{d\Delta i_d}{dt} = \frac{1}{L} (-E_0 \sin \delta_0 \Delta \delta + \Delta E \cos \delta_0 - R \Delta i_d + \omega_0 L \Delta i_q) \tag{14}$$

$$\frac{d\Delta i_q}{dt} = \frac{1}{L} (E_0 \cos \delta_0 \Delta \delta + \Delta E \sin \delta_0 - R \Delta i_q + \omega_0 L \Delta i_d) \tag{15}$$

Expressions (4) and (7)-(15) represent a sixth order system and contain all the Eigen values of the multivariable multi-input multi-output controller and the connected power system.

International Journal of Innovative Research in Science, Engineering and Technology

(An ISO 3297: 2007 Certified Organization)

Website: www.ijirset.com

Vol. 6, Issue 1, January 2017

At the time of design process, even though small values of K_f and larger magnitudes of yields a high stability margin and quick response, the steady-state error is abnormally incremented particularly in weak grids with high load angle. Therefore, a load angle oscillation becomes more at the point of instability during contingencies.

The entire system model is, here u is the control input.

$$\dot{x}_1 = \dot{x}_2 \tag{16}$$

$$\dot{x}_2 = a_1 x_1 + a_2 x_2 + a_3 x_3 \tag{17}$$

$$\dot{x}_3 = u_f + E \frac{V_L}{X} x_2 \cos x_1 + \omega_v x_3 \tag{18}$$

Where $a_1 = -K_p K_d$, $a_2 = -K_p K_d K_f$ & $a_3 = -K_p$ and $[x_1 x_2 x_3] = [\Delta\delta, \Delta\omega, \Delta P]$. u_f Is described by $u_f = (u_w V_L \sin x_1)/X$, The parameters of the system are presented in Table 1.

Parameter	Value (SI units)	Parameter	Value (SI units)
VSC maximum Power Capacity	7MW	K_p	0.1
VSC voltage(L-L rms)	4160v	K_v	200
Ef-ref (phase maximum voltage)	3400v	K_{vi}	100
K_f	5	W_v	500
K_d	1e5		

Table 1: Controller Parameters

A nonlinear back-stepping power damping controller is designed and added to the linear controller to overcome the problem of weak performance and instability. The structures of the controllers are decoupled because the nonlinear controller is additional one which supplies an added signal for the linear controller.

IV. EXPERIMENTAL RESULTS

The system consists of a 7.0MW VSC, filter, local load, transformer and a bridge line connecting the VSC to the grid. Having a specific value to indicate that the impedance $0.2+j0.5\Omega$ is the equivalent impedance of the strong source referring to the spreading (distribution) level. The simulation of the system is carried out in MATLAB/SIMULINK platform. The parameters of the controller are represented in the table 1. The local load at the output terminal is provided by the DG unit and it is joined to a strong grid by means of a very lacking strength interface with total impedance of $|Z|=|R+jX|=4.4+j43.5|=43.7\Omega$. during this period , the connecting line is very nearly inductive, the power capacity of the interface line is proximate by

$$P \approx \frac{E F V_L}{X} \sin \delta_f \tag{19}$$

While notations are explained here X is total reactance of the transformer, line and strong grid. Therefore, the maximum real power transfer capacity of the joining the line is equal to

$$P_{\max} = 13880^2 / 43.5 \approx 4.44 \text{MW}$$

A wide variety of scenarios have been applied to verify the effectiveness of the proposed hybrid nonlinear controller. System performance at low- and high-power references, transition to islanding, self-synchronization, sudden deviation in grid angle and three phase fault is studied. The advantage of the proposed controller is its flexibility to work in different conditions, i.e., grid-connected and islanded modes without reconfiguration whereas the nonlinear grid synchronizer enables the plug-and-play feature. The following results can be retained from the simulation results: from sections (a) and (b) it is drawn that the controller is able to function in both low-power and high-power levels in very weak grids. The SCR of the system is equal to one and as it will be shown that the VSC can easily inject 0.85 p.u. real power to the grid while it has well damped transient performance.

International Journal of Innovative Research in Science, Engineering and Technology

(An ISO 3297: 2007 Certified Organization)

Website: www.ijirset.com

Vol. 6, Issue 1, January 2017

This is in contrast with conventional vector control which can only exchange 0.6 p.u. real power with a grid; otherwise it might face instability. The following results depict us proposed controller under different fault conditions.

➤ Lower Power Injection

A distance range of operating points is to be studied to determine the behaviour of the controller. It is to be imagined that, at the starting system supplies 80 KW, and $t=1s$, the reference power is incremented to 2.0MW.

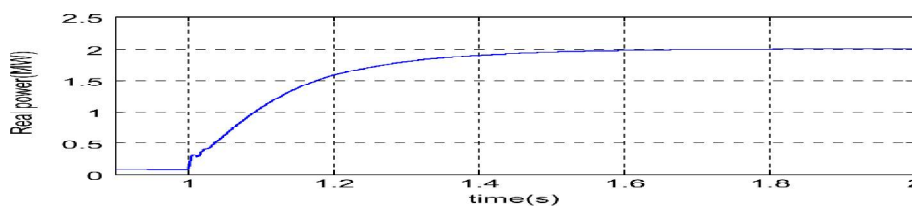


Fig. 6 Controller performance in low-power injection

The response of real power is shown in fig.6, which views a seamless transition. The rise time is about 0.6 s and perfect reference record without any overshoot.

➤ High Power Injection

The reference power is changed to 2.0MW to 6.0MW indicating closeness to the VSCs maximum power capacity at fixed voltage working and a load angle more than 1.03 rad is expected.

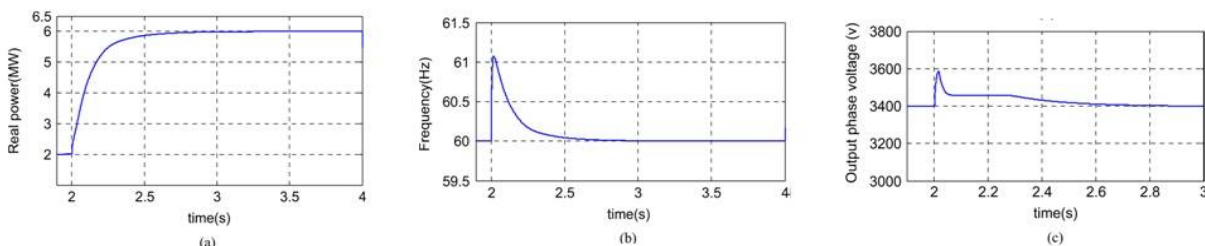


Fig. 7 Controller performance in high-power injection (a) Real power.(b) Frequency (c) Phase-voltage amplitude

Fig 7 (a) depicts the real power (b) frequency (c) output phase voltage variation waveforms as shown. It is to be noted that the response is smooth but contains a greater rise-time. The output phase voltage amplitude presents the controller performance to encourage VSCs voltage at the time of load angle variation to provide high real power injection. The general characteristics of the system which gives rise to voltage sag subsequent to increase in output power and at the same time with high voltage drop, which is a contrast.

➤ Transition to island mode

The postulated sequence that may exist in DG applications to supply local critical loads is islanded operation. At $t=4s$ the VSC is jumped to the separated mode because of fault in the grid. Reconfiguration of the system is not needed.

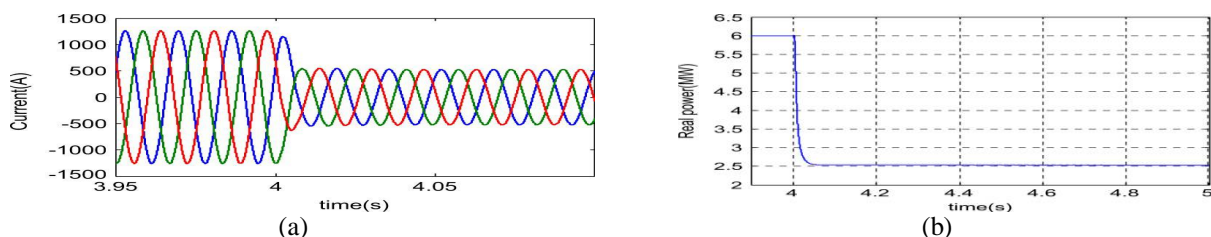


Fig. 8 Controller performance in (a) Real power during transition to islanding (b) Current waveforms subsequent to islanding

International Journal of Innovative Research in Science, Engineering and Technology

(An ISO 3297: 2007 Certified Organization)

Website: www.ijirset.com

Vol. 6, Issue 1, January 2017

Fig. 8 (a) and (b) shows the smooth transition without any unstable factors. Large steady state deviations in the grid connected mode are attained when K_f is decremented to obtain quick response. The respective current waveforms are observed which is smooth and fast transition because of the majority of the controller in either modes of operation.

➤ Self-Synchronized Grid Restoration

Powerless grids have more transients during resynchronization because of the fact that load angle is essentially large and after grid restoration moves to the nonlinear region freely.

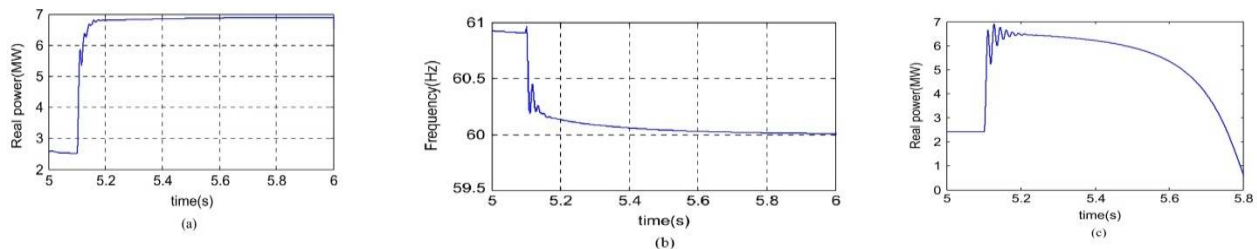


Fig. 9 System performance during grid restoration (a) Real power with nonlinear supplementary controller (b) Frequency (c) Real power without the supplementary controller

Fig 9 (a) shows the respective waveforms and depicts that the system with nonlinear controller supplies smooth and quick grid connection. The system response without using the supplementary controller is depicted in fig. 9 (b) shows that powerless grid connections cause instability. Fig. 9 (c) shows the current waveform of the system with supplementary controller depicts the well-damped characteristics even in the out-of-phase reclosing modes.

➤ Fault-Ride Through Capability: (Disturbance in the Grid Angle)

Along with the large connecting impedance, powerless grids may be affected by the sudden changes in the voltage angle and frequency.

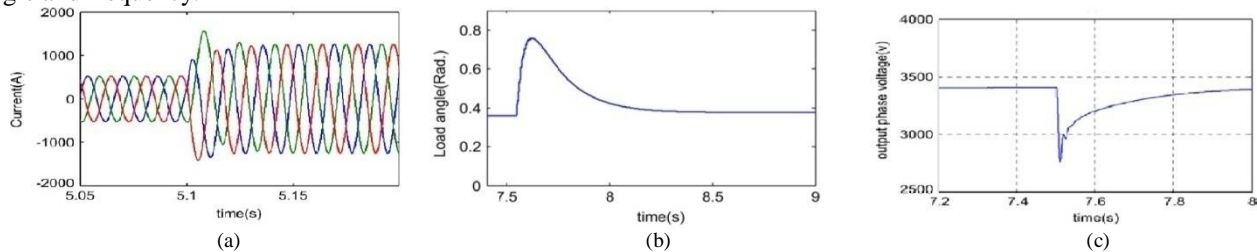


Fig. 10. System performance during disturbance grid angle (a) Current waveforms subsequent to self-synchronization with supplementary Control (b) Load angle variation (c) subsequent output voltage disturbance in the grid angle

Fig. 10 shows the resulting waveforms of the load angle and phase voltage amplitude respectively, verifies that VSC easily identifies the angle variations even under high disturbances without loss of stability and reduced performance. This is a very interesting quality of the controller where it works as a virtual PLL, and automatically monitors grid frequency and angle deviations. If we observe the waveforms in Fig. 10 (b), (c) We can justify that the output voltage amplitude is drastically decremented to keep the output power limited. The fact behind that is decrement in the grid voltage angle exhibits sudden increase in output power. Therefore, the output voltage must be decreased to maintain real power stability.

➤ Fault-Ride Through Capability: (Three Phase Fault)

The Following Fig.11 visualizes the VSC's fault-ride-through execution when a three-phase bolted fault strikes near to the end of connecting line 2. The fault is initiated at $t = 9s$ and the line 2 is separated from the grid by the guard system after 0.16s.

International Journal of Innovative Research in Science, Engineering and Technology

(An ISO 3297: 2007 Certified Organization)

Website: www.ijirset.com

Vol. 6, Issue 1, January 2017

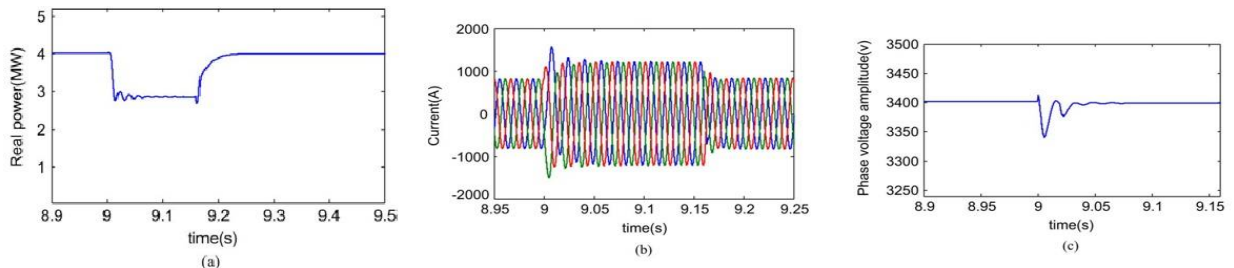


Fig. 11. System waveforms subsequent to a three-phase fault (a) Real power (b) Instantaneous current waveforms (c) Amplitude of the phase voltage

Fig.11 views the waveforms of the (a) output real power, (b) current and (c) phase voltage amplitude. From the waveforms, it is known that VSC is not subjected to over-currents during three-phase faults. At the event of fault, the real power waveform is seamless and restricted, the voltage drops and the reactive power is incremented. At $t = 9s$, the circuit breakers on both sides of the connecting line 2 becomes active and the line is separated from rest of the grid. Large signal changes occur in the system during the isolation of the connecting line.

After the separation of the line 2 at $t = 9s$, voltage, real power and current replaces back to the initial conditions before the fault but the operating points are different. This verifies the uncertainties of the system during the sudden large transients. The reconnection of the connecting line 2 is smooth and the waveforms present well-damped characteristics which can be observed.

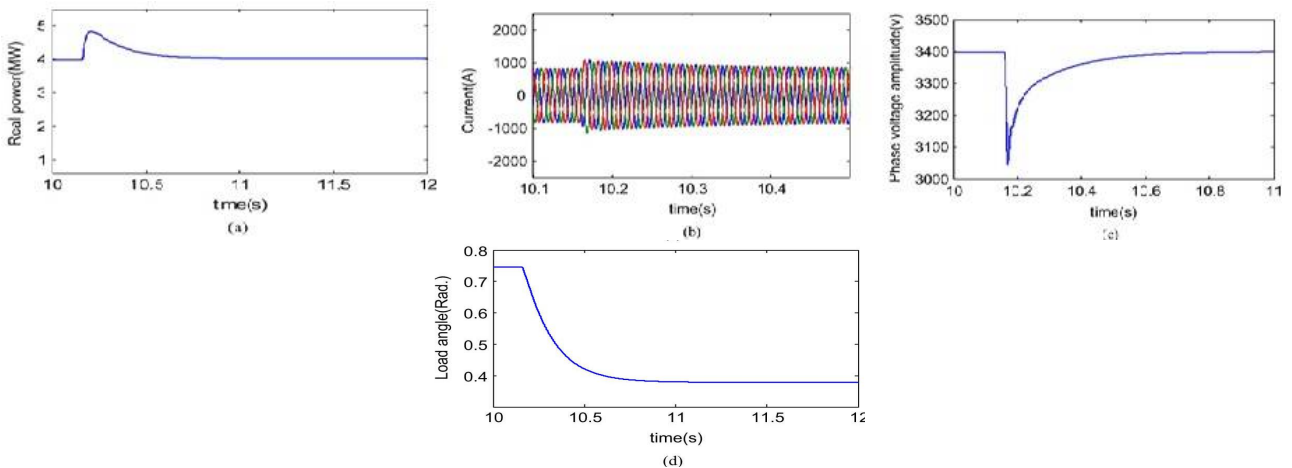


Fig. 12. System waveforms subsequent to reconnection of line 2 (a) Real power (b) Instantaneous current (c) Amplitude of the output phase-voltage (d) Load angle

If it is assumed that if the fault is cleared at $t = 10.16s$ when line 2 is again switched into the circuit. The waveform corresponding to the reconnection of line 2 are as shown in Fig.12 (a) real power, (b) current, (c) amplitude of the phase voltage and (d) load angle. When the line 2 is activated after the re-closure, the overall system settles down in 0.7s. The reconnection of connecting line 2 is smooth and all the waveforms present well-damped characteristics.

V. CONCLUSION

In this paper, a new methodology to improve the performance of the weak grids. The linear power damping controller mimics smart grids with extra power damping synchronization providing extra self-synchronization with the grid which

International Journal of Innovative Research in Science, Engineering and Technology

(An ISO 3297: 2007 Certified Organization)

Website: www.ijirset.com

Vol. 6, Issue 1, January 2017

eliminates PLL. A wide range of scenario has been applied to verify the effectiveness of the proposed linear controller. System performance under low-high references, transition to islanding, self-synchronization is studied. These cases are considered as large-signal disturbances, thus the proposed nonlinear controller can enhance system performance in these cases. Moreover, the controller is able to work in very weak grids with SCR less than 2 and supplies the rated power because of its damping and synchronizing power characteristics. The design process for the linear and nonlinear scenarios has been presented and simulation results were presented to validate the controller effectiveness.

REFERENCES

- [1] A. Guerrero et al., "Distributed generation," IEEE Ind. Electron. Mag, pp. 52–64, Mar. 2010.
- [2] N. Flourentzou, V. G. Agelidis, and G. D. Demetriades, "VSC-based HVDC power transmission systems: An overview," IEEE Trans. Power Electron., vol. 24, no. 3, pp. 592–602, Mar. 2009.
- [3] B. Parkhideh and S. Bhattacharya, "Vector-controlled voltage-source converter- based transmission under grid disturbances," IEEE Trans. Power Electron. vol. 28, no. 2, pp. 661–672, 2012.
- [4] Y.-P. Ding and J.-H. Liu, "Study on vector control used in VSC-HVDC," in Proc. IEEE Power Engineering and Automation Conf. (PEAM), 2011.
- [5] T. Noguchi, H. Tomiki, S. Kondo, and I. Takahashi, "Direct power control of PWM converter without power-source voltage sensors," IEEE Trans. Ind. Applicant. vol. 34, no. 3, pp. 473–479, May/Jun. 1998.
- [6] J. Verwecken, F. Silva, D. Barros, and J. Driesen, "Direct power control of series converter of unified power-flow controller with three-level neutral point clamped converter," IEEE Trans. Power Del., vol. 27, no. 4, pp. 1772–1782, Oct. 2012.
- [7] F. Blaabjerg, R. Teodorescu, M. Liserre, and A. V. Timbus, "Overview of control and grid synchronization for distributed power generation systems," IEEE Trans. Ind. Electron., vol. 53, no. 5, pp. 1398–1408, Oct. 2006.
- [8] L. Zhang, L. Harnefors, and H. -P. Nee, "Power-synchronization control of grid-connected voltage-source converters," IEEE Trans. Power Syst., vol. 25, no. 2, pp. 809–819, May 2010.
- [9] Q. -C. Zhong, P. -L. Nguyen, Z. Ma, and W. Sheng, "Self-synchronized Synchronverter: inverters without a dedicated synchronization unit," IEEE Trans. Power Electron., vol. 29, no. 2, pp. 617–630, 2014.
- [10] L. Zhang, L. Harnefors, and H. -P. Nee, "Modeling and control of VSCHVDC links connected to island systems," IEEE Trans. Power Syst., vol. 26, no. 2, pp. 783–793, May 2011.
- [11] L. Zhang, L. Harnefors, and H. -P. Nee, "Analysis of stability limitations of a VSC-HVDC link using power-synchronization control," IEEE Trans. Power Syst., vol. 26, no. 3, pp. 1326–1336, Aug. 2011.